Received: 1 October 2017 | Revised: 28 January 2018 | Accepted: 11 April 2018

DOI: 10.1002/ima.22275

RESEARCH ARTICLE

WILEY

Convex MR brain image reconstruction via non-convex total variation minimization

Yilin Liu | **Huiqian Du** | **Zexian Wang** | **Wenbo Mei**

School of Information and Electronics, Beijing Institute of Technology, Beijing 100081, China

Correspondence
Huiqian Du, School of Information and Electronics, Beijing Institute of Technology, Beijing 100081, China.
Email: duhuiqian@bit.edu.cn

Abstract

Total variation (TV) regularization is a technique commonly utilized to promote sparsity of image in gradient domain. In this article, we address the problem of MR brain image reconstruction from highly undersampled Fourier measurements. We define the Moreau enhanced function of L_1 norm, and introduce the minmax-concave TV (MCTV) penalty as a regularization term for MR brain image reconstruction. MCTV strongly induces the sparsity in gradient domain, and fits the frame of fast algorithms (eg, ADMM) for solving optimization problems. Although MCTV is non-convex, the cost function in each iteration step can maintain convexity by specifying the relative nonconvexity parameter properly. Experimental results demonstrate the superior performance of the proposed method in comparison with standard TV as well as nonlocal TV minimization method, which suggests that MCTV may have promising applications in the field of neuroscience in the future.

KEYWORDS

brain image reconstruction, magnetic resonance imaging, non-convex regularization, total variation

1 | INTRODUCTION

Magnetic resonance imaging (MRI) is an approach broadly used for clinical diagnosis because of its ability to effectively depict soft tissue changes, and its noninvasiveness. One of the primary limiting factor of MRI application is its relatively slow acquisition time for imaging. To speed up scanning, reducing data acquisition quantity without degrading reconstruction quality has always been the focus.

Recently proposed compressed sensing (CS) theory states that it is possible to reconstruct a sparse signal exactly from a small number of random measurements by exploiting its sparsity in some transform domains (eg, wavelet, gradient, Fourier, etc).[1,2] This theory makes reconstructing MR brain images from highly undersampled k-space data possible, and becomes the foundation of several reconstruction methods.[3–5] Most CS-based reconstruction methods adopt the total variation (TV),[6] or generalized TV form as a regularization term to promote the sparsity in gradient domain. Standard TV is based solely on local, first order derivative features. It is defined as L_1 norm of gradient, and has desirable properties such as convexity and the ability to preserve edges. High order TV takes second order derivatives into account.[7] Total Generalized Variation (TGV) of second order balances between the first and second order derivative of functions.[8] Nonlocal TV (NLTV) imposes nonuniform weight on a more global area centered on each pixel.[9]

All of the above TV adopt L_1 norm instead of L_0 norm, because L_0 norm is non-convex. When L_0 norm is used, there is no guarantee that global minimizers exist, and it is very difficult to find global minimizers. L_1 norm, conversely, enhances sparsity most effectively among convex functions. But L_1 norm as a penalty tends to underestimate signal values, and it is not a very good proxy of L_0 norm. Thus, a variety of non-convex penalties were designed to outperform L_1 norm regularization for sparse approximation,[10–17] and some of them can maintain convexity of the cost function. For example, Selesnick defined Moreau-enhanced TV in his paper,[10] and applied it to onedimensional signal denoising problem. However, this TV form is not a practical choice for MR brain image reconstruction, since it is hard to develop a corresponding fast algorithm which can solve the two-dimensional (2D)

optimization problem. In this article, we give the definition of Moreau enhanced function, and introduce minmax-concave (MC) penalty as a special case of Moreau enhanced function. Then we apply the finite difference operator D to MC penalty to introduce MCTV. The advantage of MCTV is that it is a good proxy of L_0 norm so that it can strongly induce sparsity of gradient, and this new form allows us to use fast algorithms such as ADMM to efficiently reconstruct 2D brain images. Although MCTV penalty is non-convex, by specifying the nonconvexity parameter properly, the cost function in each iteration will maintain convexity. Experimental results on real MR brain images demonstrate that the proposed method outperforms standard TV as well as NLTV minimization method.

This article will proceed as follows. Section 2 introduces Moreau envelope, Moreau enhanced function and MCTV. Section 3 gives details of the proposed method and the fast algorithm to solve it. In Section 4, a series of experimental results is given to demonstrate the effectiveness of MCTV in MR brain image reconstruction. Finally, the conclusions are drawn in Section 5.

2 | MOREAU ENHANCED FUNCTION AND MCTV

In this section, we will first give the definition of Moreau envelope, and define Moreau enhanced function. Second, we will introduce MC penalty and define MCTV. Finally, we will explain why MCTV has potential to enhance gradient sparsity further compared to standard and some other non-convex TV penalty.

Definition 1 Let $\alpha \geq 0$, $S_\alpha : R^N \to R$ is defined as Moreau envelope of function f.[10,18]

$$S_\alpha(\boldsymbol{x}) = \min_{\boldsymbol{v}} \left\{ \frac{\alpha}{2} ||\boldsymbol{x}-\boldsymbol{v}||_2^2 + f(\boldsymbol{v}) \right\} \tag{1}$$

Definition 2 Let $\alpha \geq 0$, we define $M_\alpha : R^N \to R$ as Moreau enhanced function of function f.

$$M_\alpha(\boldsymbol{x}) = f(\boldsymbol{x}) - S_\alpha(\boldsymbol{x}) \tag{2}$$

For function $f(\boldsymbol{x}) = ||\boldsymbol{x}||_1$, we denote the Moreau enhanced function of it as $\phi_\alpha(\boldsymbol{x})$: $R^N \to R$ with the following form:

$$\phi_\alpha(\boldsymbol{x}) = ||\boldsymbol{x}||_1 - \min_{\boldsymbol{v}} \left\{ \frac{\alpha}{2} ||\boldsymbol{x}-\boldsymbol{v}||_2^2 + ||\boldsymbol{v}||_1 \right\} \tag{3}$$

$\phi_\alpha(\boldsymbol{x})$ can also be expressed in a pointwise way as

$$\phi_\alpha(\boldsymbol{x}) = \sum_{i=1}^{N} \varphi_{MC\_\alpha}(x_i) \tag{4}$$

and

$$\varphi_{MC\_\alpha}(x) = |x| - \min_{v} \left\{ \frac{\alpha}{2}(x-v)_2^2 + |v| \right\} \tag{5}$$

where $x \in R$. As shown in Ref. 19, the solution of $\min_v \left\{ \frac{\alpha}{2}(x-v)_2^2 + |v| \right\}$ is Huber function $H_\alpha(x)$:

$$H_\alpha(x) = \begin{cases} \dfrac{1}{2\alpha}x^2 & |x| \leq \alpha \\ |x| - \dfrac{\alpha}{2} & |x| > \alpha \end{cases} \tag{6}$$

Then $\varphi_{MC\_\alpha}(x)$ can be written as

$$\varphi_{MC\_\alpha}(x) = \begin{cases} |x| - \dfrac{1}{2\alpha}x^2 & |x| \leq \alpha \\ \dfrac{\alpha}{2} & |x| > \alpha \end{cases} \tag{7}$$

which is the MC penalty.[20]

Next, we will show $\phi_\alpha(\boldsymbol{x})$ is a good proxy of L_0 norm comparing with other functions. L_0 norm of $\boldsymbol{x}$ is defined as the number of nonzero elements of $\boldsymbol{x}$: $||\boldsymbol{x}||_0 = \sum_{i=1}^{N} g_0(x_i)$, where

$$g_0(x) = \begin{cases} 0 & x = 0 \\ 1 & otherwise \end{cases} \tag{8}$$

L_1 norm of $\boldsymbol{x}$ is $||\boldsymbol{x}||_1 = \sum_{i=1}^{N} g_1(x_i)$, where

$$g_1(x) = |x| \tag{9}$$

In Figure 1, we plotted the curves of function $g_0(x)$, $g_1(x)$, $\varphi_{\exp\_\alpha}(x)$ ($\alpha = 1$) and $\varphi_{MC\_\alpha}(x)$ ($\alpha = 2$). $\varphi_{\exp\_\alpha}(x)$ is defined as

$$\varphi_{\exp\_\alpha}(x) = \frac{1 - e^{-\alpha|x|}}{\alpha} \tag{10}$$

It was proposed by Lanza in Ref. 16 very recently and applied to 2D image denoising. Compared with $g_1(x)$ and $\varphi_{\exp\_\alpha}(x)$, $\varphi_{MC\_\alpha}(x)$ is closer to $g_0(x)$ by selecting proper value of nonconvexity parameter α. Therefore, $\phi_\alpha(\boldsymbol{x})$ is a good proxy of L_0 norm.

Considering most MR brain images are not sparse but demonstrate piecewise constant behavior in spatial domain, we intend to promote sparsity in gradient domain. To do so, we replace $\boldsymbol{x}$ with its gradient $D\boldsymbol{x}$ in Equation 3 (D is finite difference operator), which leads to our definition of MCTV below.

Definition 3 Let $\alpha \geq 0$, $||\boldsymbol{x}||_{\mathrm{MCTV}}$: $R^N \to R$ is defined as MCTV of $\boldsymbol{x}$.

$$||\boldsymbol{x}||_{\mathrm{MCTV}} = \phi_\alpha(D\boldsymbol{x}) = ||D\boldsymbol{x}||_1 - \min_{\boldsymbol{v}} \left\{ \frac{\alpha}{2} ||D\boldsymbol{x}-\boldsymbol{v}||_2^2 + ||\boldsymbol{v}||_1 \right\} \tag{11}$$

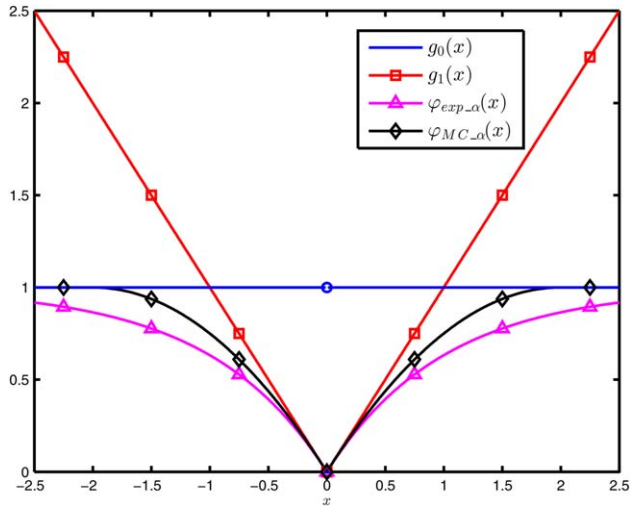

FIGURE 1 Curves of function $g_0(x)$, $g_1(x)$, $\varphi_{\exp\_\alpha}(x)$ ($\alpha=1$) and $\varphi_{MC\_\alpha}(x)$ ($\alpha=2$) [Color figure can be viewed at wileyonlinelibrary.com]

If $\boldsymbol{x}$ is a vector, then $(D\boldsymbol{x})_i=(x_{i+1}-x_i)$.
If $\boldsymbol{x}$ is an image, then $(D\boldsymbol{x})_{i,j}=(x_{i+1,j}-x_{i,j}, x_{i,j+1}-x_{i,j})$. We can see that $\boldsymbol{v}$ is the approximation to $D\boldsymbol{x}$.

In the next section, we will demonstrate that the form of MCTV allows us to develop a corresponding fast algorithm based on ADMM, which facilitates its application in MR brain image reconstruction.

3 | MR BRAIN IMAGE RECONSTRUCTION VIA MCTV REGULARIZATION

In this section, we will propose a new method for MR brain image reconstruction via MCTV minimization. A new reconstruction model will be given first, then we will develop a simple and fast algorithm based on ADMM to solve the proposed optimization problem.

3.1 | Proposed model

In the field of MRI, the data acquisition is commonly modeled as

$$\boldsymbol{y}=RF\boldsymbol{x}+\boldsymbol{w} \tag{12}$$

where $\boldsymbol{x}$ is the desired MR brain image, R denotes the undersampling operator, and F represents the Fourier operator; $\boldsymbol{w}$ is noise or disturbance and $\boldsymbol{y}$ is the undersampled Fourier measurement. The scale of $\boldsymbol{y}$ is much less than that of $\boldsymbol{x}$.

For CS based image reconstruction, it is very common to search for the reconstruction result by minimizing the following function with standard TV regularization term.

$$\hat{\boldsymbol{x}}=\arg\min_x\left\{\frac{1}{2}||\boldsymbol{y}-RF\boldsymbol{x}||_2^2+\lambda||\boldsymbol{x}||_{\mathrm{TV}}\right\} \tag{13}$$

where $||\boldsymbol{x}||_{\mathrm{TV}}=||D\boldsymbol{x}||_1$.

Since MCTV promotes the gradient sparsity more effectively than standard TV, we propose to reconstruct $\boldsymbol{x}$ by using MCTV as a regularization term as follows.

$$\hat{\boldsymbol{x}}=\arg\min_x\left\{\frac{1}{2}||\boldsymbol{y}-RF\boldsymbol{x}||_2^2+\lambda||\boldsymbol{x}||_{\mathrm{MCTV}}\right\} \tag{14}$$

3.2 | Algorithm

In accordance with the definition of $||\boldsymbol{x}||_{\mathrm{MCTV}}$, we formulate problem (14) into the form below.

$$\arg\min_x\left\{\frac{1}{2}||\boldsymbol{y}-RF\boldsymbol{x}||_2^2+\lambda\left(||D\boldsymbol{x}||_1-\min_v\left\{\frac{\alpha}{2}||D\boldsymbol{x}-\boldsymbol{v}||_2^2+||\boldsymbol{v}||_1\right\}\right)\right\} \tag{15}$$

The penalty is non-convex, but the algorithm we develop below shows that the cost function in each iteration maintains its convexity if we specify the nonconvexity parameter α properly.

Set $\boldsymbol{z}=D\boldsymbol{x}$, then the augmented Lagrangian form of (15) is given by

$$\mathrm{L}(\boldsymbol{x},\boldsymbol{z},\boldsymbol{u})=\frac{1}{2}||\boldsymbol{y}-RF\boldsymbol{x}||_2^2+\lambda\phi_\alpha(\boldsymbol{z})-\lambda u^T(\boldsymbol{z}-D\boldsymbol{x})+\frac{\lambda\rho}{2}||\boldsymbol{z}-D\boldsymbol{x}||_2^2 \tag{16}$$

where $\phi_\alpha(\boldsymbol{z})$ is defined in Equation 3.

According to ADMM,[21] the minimizer of function (16) can be found by solving the following sub-problems.

Step 1. Update $\boldsymbol{x}^{k+1}$ with $\boldsymbol{z}^k$ and $\boldsymbol{u}^k$ fixed:

$$\boldsymbol{x}^{k+1}=\arg\min_x\left\{\frac{1}{2}||\boldsymbol{y}-RF\boldsymbol{x}||_2^2+\lambda\left(\boldsymbol{u}^k\right)^TD\boldsymbol{x}+\frac{\lambda\rho}{2}||\boldsymbol{z}^k-D\boldsymbol{x}||_2^2\right\} \tag{17}$$

The optimal solution is given below.

$$\left(F^TR^TRF+\lambda\rho D^TD\right)\boldsymbol{x}^{k+1}=(RF)^T\boldsymbol{y}+\lambda\rho D^T\boldsymbol{z}^k-\lambda D^T\boldsymbol{u}^k \tag{18}$$

For simplicity, we set $\boldsymbol{q}^k=(RF)^T\boldsymbol{y}+\lambda\rho D^T\boldsymbol{z}^k-\lambda D^T\boldsymbol{u}^k$. Since $F^T=F^{-1}$, the equation above can be written as

$$F^{-1}\left(R^TR+\lambda\rho F\left(D^TD\right)F^{-1}\right)F\boldsymbol{x}^{k+1}=\boldsymbol{q}^k \tag{19}$$

Since D^TD is circulant, it can be diagonalized by Fourier transform. Set $Q=R^TR+\lambda\rho F(D^TD)F^{-1}$, Q is diagonal, Equation 19 can be written as

$$F^{-1}QF\boldsymbol{x}^{k+1}=\boldsymbol{q}^k \tag{20}$$

Then we can find the optimal value of $\boldsymbol{x}^{k+1}$ using two Fourier transforms.

$$\boldsymbol{x}^{k+1}=F^{-1}Q^{-1}F\boldsymbol{q}^k \tag{21}$$

Since Q is diagonal, Q^{-1} can be obtained conveniently via element-wise division.

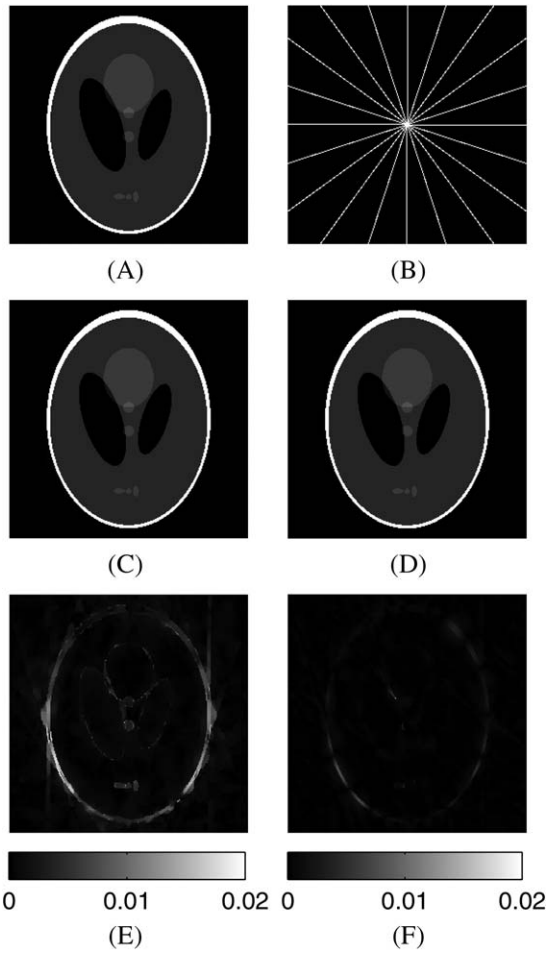

FIGURE 2 A, Original image (Shepp Logan); B, the radial sampling trajectory with 10 lines; C, the reconstructed image using standard TV penalty; D, the reconstructed image using MCTV penalty; E, difference between (A) and (C); F, difference between (A) and (D)

Step 2. Update z^{k+1} with $\boldsymbol{x}^{k+1}$ and $\boldsymbol{u}^k$ fixed:

$$z^{k+1} = \arg\min_z \left\{ \lambda\phi_\alpha(z) - \lambda\left(\boldsymbol{u}^k\right)^T z + \frac{\lambda\rho}{2}||z - D\boldsymbol{x}^{k+1}||_2^2 \right\}$$
$$= \arg\min_z \left\{ \phi_\alpha(z) + \frac{\rho}{2}\left|\left|z - \left(D\boldsymbol{x}^{k+1} + \frac{\boldsymbol{u}^k}{\rho}\right)\right|\right|_2^2 \right\} \quad (22)$$

The value of the nonconvexity parameter α controls the convexity of the cost function as shown in Theorem 1.

Theorem 1 *Let* $\lambda > 0$, $\alpha > 0$, *define* $G_\alpha(\boldsymbol{x})$ *as*

$$G_\alpha(\boldsymbol{x}) = \frac{1}{2}||\boldsymbol{y} - \boldsymbol{x}||_2^2 + \lambda\phi_\alpha(\boldsymbol{x}) \quad (23)$$

If $0 \le \alpha \le \frac{1}{\lambda}$, *then* $G_\alpha(\boldsymbol{x})$ *is convex.*

Proof :

$$G_\alpha(\boldsymbol{x}) = \frac{1}{2}||\boldsymbol{y} - \boldsymbol{x}||_2^2 + \lambda\left\{||\boldsymbol{x}||_1 - \min_v \left(\frac{\alpha}{2}||\boldsymbol{x} - \boldsymbol{v}||_2^2 + ||\boldsymbol{v}||_1\right)\right\}$$
$$= \max_v \left\{ \frac{1}{2}||\boldsymbol{y} - \boldsymbol{x}||_2^2 + \lambda||\boldsymbol{x}||_1 - \lambda||\boldsymbol{v}||_1 - \frac{\lambda\alpha}{2}||\boldsymbol{x} - \boldsymbol{v}||^2 \right\} \quad (24)$$
$$= \frac{1}{2}(1 - \lambda\alpha)||\boldsymbol{x}||_2^2 + \lambda||\boldsymbol{x}||_1 + \max_v \; g(\boldsymbol{x}, \boldsymbol{v})$$

■

$g(\boldsymbol{x}, \boldsymbol{v})$ is the affine function of $\boldsymbol{x}$, it is convex since it is the pointwise maximum of a set of convex functions. Therefore, $G_\alpha(\boldsymbol{x})$ is a convex function if $1 - \lambda\alpha \ge 0$, or $0 \le \alpha \le \frac{1}{\lambda}$.

Based on Theorem 1, if $\alpha \le \rho$, the cost function in (22) maintains its convexity. From the reference,[10] it is easy to understand that by specifying the value of parameter α as $\alpha \le \rho$, the z^{k+1} generated by Equation 26 converges to the solution of optimization problem (22). We write the iteration procedure below.

Do

$$\boldsymbol{t}^k = D\boldsymbol{x}^{k+1} + \frac{\boldsymbol{u}^k}{\rho} + \frac{\alpha}{\rho}\left(z^k - l_1\left(z^k; \frac{1}{\alpha}\right)\right) \quad (25)$$

$$z^{k+1} = l_1\left(\boldsymbol{t}^k; \frac{1}{\rho}\right) \quad (26)$$

where

$$l_1(\boldsymbol{y}; \lambda) = \arg\min_x \left\{ \frac{1}{2}||\boldsymbol{y} - \boldsymbol{x}||_2^2 + \lambda||\boldsymbol{x}||_1 \right\} \quad (27)$$

Optimization problem (27) can be efficiently solved by Iterative Shrinkage Threshold Algorithm (ISTA).[22,23]

Step 3. Update $\boldsymbol{u}^{k+1}$ with $\boldsymbol{x}^{k+1}$ and z^{k+1} fixed:

$$\boldsymbol{u}^{k+1} = \boldsymbol{u}^k + \left(D\boldsymbol{x}^{k+1} - z^{k+1}\right) \quad (28)$$

A brief summary of the proposed algorithm is given in Algorithm 1.

Algorithm 1

Input Measurement $\boldsymbol{y} = RF\boldsymbol{x} + \boldsymbol{w}$
1. **Initialize** $\boldsymbol{x}^0 = 0$, $z^0 = 0$, $\boldsymbol{u}^0 = 0$
2. **Initialize** $\lambda > 0, \rho > 0, 0 \le \alpha \le \rho, \delta_1 > 0, \delta_2 > 0$
3. **Do while** $||\boldsymbol{x}^{k+1} - \boldsymbol{x}^k||_2 > \delta_1$
4. $\boldsymbol{q}^k = (RF)^T\boldsymbol{y} + \lambda\rho D^T z^k - \lambda D^T\boldsymbol{u}^k$
5. $Q = R^T R + \lambda\rho F(D^T D)F^{-1}$
6. $\boldsymbol{x}^{k+1} = F^{-1}Q^{-1}F\boldsymbol{q}^k$
7. **Do while** $||z^{k+1} - z^k||_2 > \delta_2$
8. $\boldsymbol{p}^k = \arg\min_p \left\{\frac{1}{2}||\boldsymbol{p} - z^k||_2^2 + \frac{1}{\alpha}||\boldsymbol{p}||_1\right\}$
9. $\boldsymbol{t}^k = D\boldsymbol{x}^{k+1} + \frac{\boldsymbol{u}^k}{\rho} + \frac{\alpha}{\rho}\left(z^k - \boldsymbol{p}^k\right)$
10. $z^{k+1} = \arg\min_z \left\{\frac{1}{2}||z - \boldsymbol{t}^k||_2^2 + \frac{1}{\rho}||z||_1\right\}$
11. **End Do**
12. $\mathbf{u}^{k+1} = \mathbf{u}^k + \left(D\mathbf{x}^{k+1} - \mathbf{z}^{k+1}\right)$
13. **End Do**

Output reconstructed image $\boldsymbol{x}$

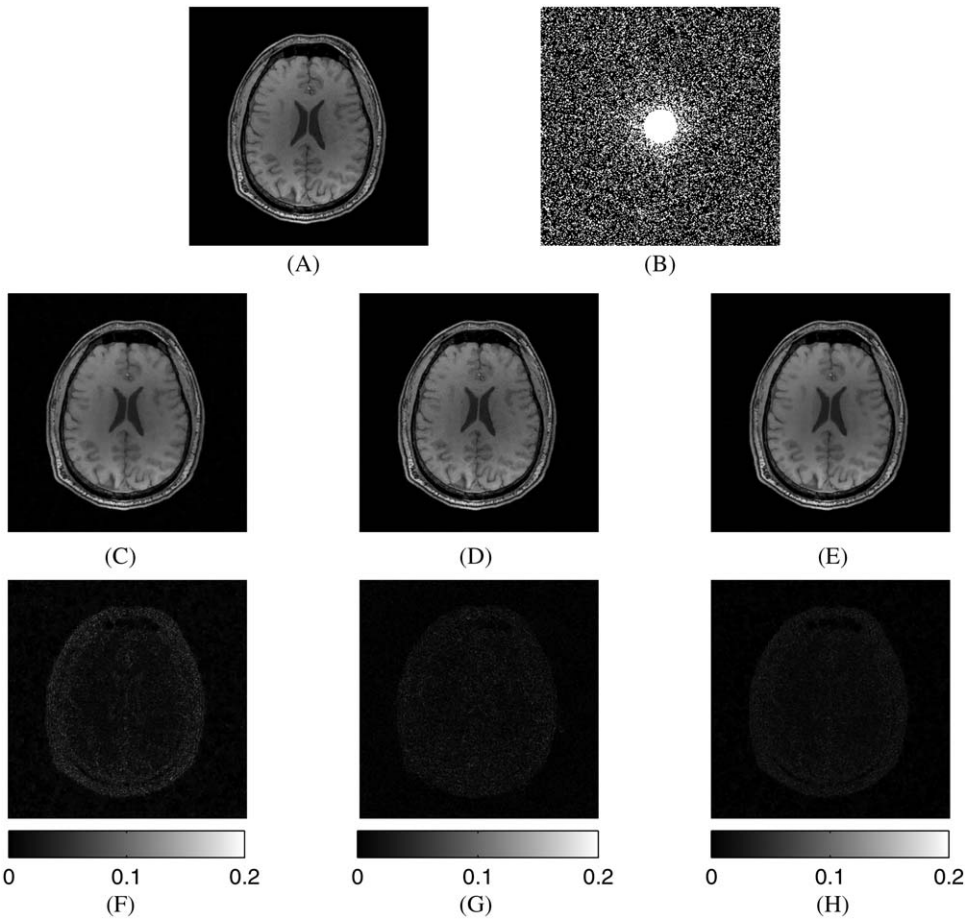

FIGURE 3 A, Original image (Brain_1); B, the undersampling template with 30% sampling rate and 0.1 sampling radius; C, the reconstructed image using standard TV penalty; D, the reconstructed image using NLTV penalty; E, the reconstructed image using MCTV penalty; F, difference between (A) and (C); G, difference between (A) and (D); H, difference between (A) and (E)

Standard TV reconstruction problem in (13) can also be solved efficiently with ADMM.[24] The whole process is similar to the proposed algorithm. The difference is, instead of calculating line 7 to line 11, standard TV minimization solves the following problem

$$z^{k+1} = \arg\min_{z} \left\{ ||z||_1 + \frac{\rho}{2} \left| \left| z - \left(D\boldsymbol{x}^{k+1} + \frac{\boldsymbol{u}^k}{\rho} \right) \right| \right|_2^2 \right\} \quad (29)$$

As presented in Algorithm 1, due to the form of MCTV, the proposed reconstruction problem can be decomposed into several sub-problems. For each subproblem, the cost function maintains its convexity in the iteration step, and can be solved effectively and conveniently. Thus, the whole algorithm is of great practical application.

4 | EXPERIMENTAL RESULTS

In this section, we will present experimental results of the proposed method, and compare them with standard TV[24] and NLTV reconstruction.[25] All of our experiments were implemented on MATLAB R2014a on a PC equipped with a 1.7 GHz CPU and 8 GB RAM. The quality and accuracy of reconstructed images were evaluated by the peak signal-to-noise ratio (PSNR) and the relative error (Err). We adopted three undersampling templates: the variable density, the radial and the Cartesian undersampling templates to prove the versatility of MCTV-based model.

First we chose the Shepp Logan phantom (256 × 256) to test the effectiveness of the proposed method. The reconstruction result was compared with standard TV. A radial sampling trajectory with 10 lines was employed, and the parameters were $\lambda = \delta_1 = \delta_2 = 0.0001$, $\rho = 50$. The value of α was chosen as $\alpha = 0.05$ $\rho = 2.5$ in MCTV to maintain the convexity of the cost function. The result was shown in Figure 2. The Err of reconstructed images of standard TV and MCTV penalty were 0.78% and 0.14%, and the PSNR of two methods were 54.3 dB and 69.3 dB, respectively.

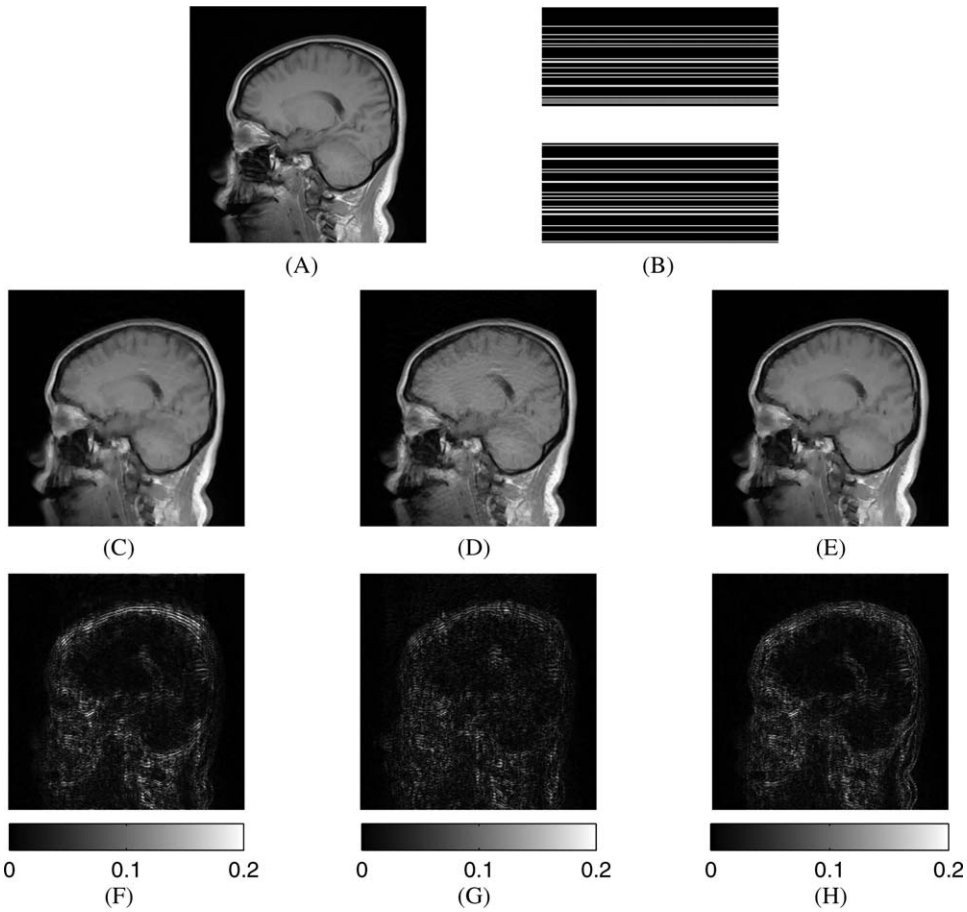

FIGURE 4 A, Original image (Brain_2); B, the Cartesian template with 70 read out lines; C, the reconstructed image using standard TV penalty; D, the reconstructed image using NLTV penalty; E, the reconstructed image using MCTV penalty; F, difference between (A) and (C); G, difference between (A) and (D); H, difference between (A) and (E)

Second, we tested the proposed method on two MR brain images with the size of 256 × 256 and compared the results with standard TV as well as NLTV. The set value of parameters in NLTV was chosen based on the suggestions given by Zhang.[25] For Brain_1, k-space data were measured using a variable density template under 30% sampling rate. The reconstruction results and the error images were shown in Figure 3. The parameters were $\lambda = \delta_1 = \delta_2 = 0.0001$, $\rho = 150$. The value of α in MCTV was chosen as $\alpha = 0.05$ $\rho = 7.5$. In Figure 5, we plotted the curves of Err versus the sampling rate. For Brain_2, the image was measured using a Cartesian template, k-space data were randomly undersampled along the phase encoding direction only with 70 lines, while keeping the frequency encoding direction fully sampled. The parameters were $\lambda = \delta_1 = \delta_2 = 0.0001$, $\rho = 150$. The value of α was chosen as $\alpha = 0.05$ $\rho = 7.5$ in MCTV. The reconstruction results and the error images were shown in Figure 4. We can see that our method can reconstruct the smooth area better than standard TV as well as NLTV in both brain images.

In Table 1, the Err and PSNR of Brain_1 and Brain_2 were listed under 30% sampling rate for the variable density template, and 70 readout lines for the Cartesian template. All the results demonstrate that MCTV outperforms standard TV and NLTV in MR brain image reconstruction.

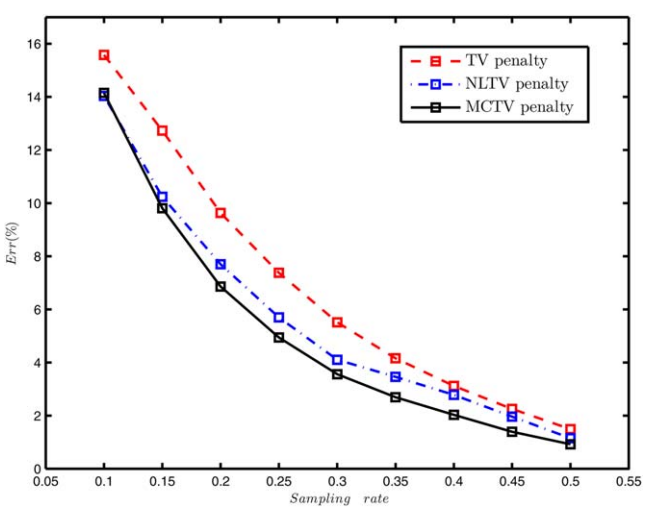

FIGURE 5 The Err versus the sampling rate [Color figure can be viewed at wileyonlinelibrary.com]

TABLE 1 Reconstruction results

Template	Image	Regularization	Err (%)	PSNR (dB)
The variable density with 30% sampling rate and 0.1 sampling radius	Brain_1	TV	5.57	35.9798
		NLTV	4.10	38.6444
		MCTV	3.61	39.7445
	Brain_2	TV	4.15	35.8730
		NLTV	3.83	36.5682
		MCTV	3.59	37.1177
The Cartesian template with 70 readout lines	Brain_1	TV	11.43	29.7376
		NLTV	10.11	30.6927
		MCTV	9.51	31.3368
	Brain_2	TV	7.09	31.2097
		NLTV	6.41	32.0384
		MCTV	6.39	32.1129

5 | CONCLUSION

We give the general definition of Moreau enhanced function, introduce MCTV, and apply it in MR brain image reconstruction. MCTV has a form which fits fast algorithm ADMM and can maintain the convexity of the cost function in each iteration. A series of experimental results demonstrates that MCTV penalty has the ability to enhance the gradient sparsity of MR brain images further compared to standard TV as well as NLTV, which allows people to use lower sampling rate in brain imaging and obtain the same or better reconstruction results in the field of neuroscience. Also it may have promising applications for clinical diagnosis in the future.

ORCID

Yilin Liu http://orcid.org/0000-0002-2828-774X

REFERENCES

[1] Candes EJ, Romberg, J, Tao T. Robust uncertainty principles: exact signal reconstruction from highly incomplete frequency information. *IEEE Trans Inform Theory.* 2006; 52:489–509.

[2] Candes EJ, Wakin MB. An introduction to compressive sampling. *IEEE Signal Process Mag.* 2008;25:21–30.

[3] Lustig M, Donoho D, Santos J, Pauly J. Compressed sensing MRI. *IEEE Signal Process Mag.* 2008;25:72–82.

[4] Lustig M, Donoho D, Pauly J. Sparse MRI: the application of compressed sensing for rapid MR imaging. *Mag Reson Med.* 2007;58:1182–1195.

[5] Herman M, Strohmer T. High-resolution radar via compressed sensing. *IEEE Trans Signal Process.* 2009;57:2275–2284.

[6] Rudin LI, Osher S, Fatemi E. Nonlinear total variation based noise removal algorithms. *Physica D: Nonlinear Phenomena.* 1992;60:259–268.

[7] Xie W-S, Yang Y-F, Zhou B. An ADMM algorithm for second-order TV-based MR image reconstruction. *Numer Algorithms.* 2014;67:827–843.

[8] Knoll F, Bredies K, Pock T, Stollberger R. Second order total generalized variation (TGV) for MRI. *Magn Reson Med.* 2011; 65:480–491.

[9] Kim H, Chen J, Wang A, Chuang C, Held M, Pouliot J. Non-local total-variation (NLTV) minimization combined with reweighted L_1-norm for compressed sensing CT reconstruction. *Phys Med Biol.* 2016;61:6878–6891.

[10] Selesnick I. Total variation denoising via the Moreau envelope. *IEEE Signal Process Lett.* 2017;24:216–220.

[11] Selesnick I, Farshchian M. Sparse signal approximation via non-separable regularization. *IEEE Trans Signal Process.* 2017;65: 2561–2575.

[12] Selesnick I, Parekh A, Bayram I. Convex 1-D total variation denoising with non-convex regularization. *IEEE Signal Process Lett.* 2015;22:141–144.

[13] Candès EJ, Wakin MB, Boyd SP. Enhancing sparsity by reweighted L_1 minimization. *Fourier Anal Appl.* 2008;14:877–905.

[14] Chen L, Gu Y. The convergence guarantees of a non-convex approach for sparse recovery. *IEEE Trans Signal Process.* 2014; 62:3754–3767.

[15] Chartrand R. Shrinkage mappings and their induced penalty functions. In 2014 Proceedings of IEEE International Conference Acoustics, Speech, Signal Process (ICASSP); 2014:1026–1029.

[16] Lanza, A, Morigi S, Sgallari F. Convex image denoising via non-convex regularization with parameter selection. *J Math Imaging Vis.* 2016;56:195–220.

[17] Lanza A, Morigi S, Sgallari F. Convex image denoising via non-convex regularization. *International Conference on Scale Space and Variational Methods in Computer Vision. Cham: Springer;* 2015:666–677.

[18] Moreau JJ. Inf-convolution des fonctions numériques sur un espace vectoriel. *C R Acad Sci Paris.* 1963;256:5047–5049.

[19] Selesnick I. Sparse regularization via convex analysis. *IEEE Trans Signal Process.* 2017;65:4481–4494.

[20] Zhang C-H. Nearly unbiased variable selection under minimax concave penalty. *Ann Stat.* 2010;38:894–942.

[21] Boyd S, Parikh N, Chu E, Peleato B, Eckstein J. Distributed optimization and statistical learning via the alternating direction method of multipliers. *Foundations Trends Machine Learning.* 2010;3:1–122.

[22] Daubechies I, Defrise M, De Mol C. An iterative thresholding algorithm for linear inverse problems with a sparsity constraint. *Commun Pure Appl Math.* 2004;57:1413–1457.

[23] Beck A, Teboulle M. A fast iterative shrinkage-thresholding algorithm for linear inverse problems. *SIAM J Imaging Sci.* 2009;2:183–202.

[24] Yang J, Zhang Y, Yin W. Fast alternating direction method for TVL_1-L_2 signal reconstruction from partial Fourier data. *IEEE J Sel Topics Signal Process.* 2010;4:288–297.

[25] Zhang X, Burger M, Bresson X, Osher S. Bregmanized nonlocal regularization for deconvolution and sparse reconstruction. *SIAM J Imaging Sci.* 2010;3:253–276.

How to cite this article: Liu Y, Du H, Wang Z, Mei W. Convex MR brain image reconstruction via non-convex total variation minimization. *Int J Imaging Syst Technol*. 2018;00:1–8. https://doi.org/10.1002/ima.22275